

Validation of Climate Models Using Ground-Based GNSS Observations

Gunnar Elgered, Tong Ning, Jan Johansson

Earth and Space Sciences, Chalmers University of Technology

Onsala Space Observatory, SE-43992 Onsala

e-mail: Gunnar.Elgered / Tong.Ning / Jan.Johansson@chalmers.se

Ulrika Willén, Erik Kjellström

Swedish Meteorological and Hydrological Institute, SE-60176 Norrköping

e-mail: Ulrika.Willen@smhi.se, Erik.Kjellstrom@smhi.se

Per Jarlemark, Ragne Emardson

SP Technical Research Institute of Sweden, SE-50115 Borås

e-mail: Per.Jarlemark@sp.se, Ragne.Emardson@sp.se

Tobias Nilsson

Institute of Geodesy and Geophysics, Vienna University of Technology, AT-1040 Vienna

e-mail: Tobias.Nilsson@tuwien.ac.at

Introduction

Water vapour is the most important greenhouse gas in the atmosphere. It efficiently absorbs thermal radiation in the troposphere leading to higher near-surface temperatures than what would otherwise be the case. In addition to this, water vapour plays a key role in the energy balance of the climate system by transporting heat from the surface to the atmosphere through latent heat release. Furthermore, latent heat transport is the most important process for redistributing heat from low to high latitudes.

As the water vapour content of the atmosphere is regulated by the temperature, global warming will have an impact on the atmospheric water vapour content. For each 1°C of temperature increase the water vapour content will increase by 6–7% which in turn acts to heat the climate system even more thus amplifying the change. Connected to such changes in the water vapour content are changes in the hydrological cycle, i.e. evaporation and precipitation (e.g. Bengtsson, 2010). The gradient in evaporation-precipitation increases proportionally to the lower tropospheric water vapour leading to larger differences between dry and wet areas. As a consequence, a good knowledge about the regional distribution of the water vapour content of the atmosphere — in the following referred to as Integrated Water Vapour (IWV) — is crucial as it ultimately determines the rate of precipitation.

Traditionally radiosondes and satellite observations have been used to observe the IWV. Ross & Elliott (1996) and (2001) found an upward trend in the IWV from radiosonde measurements from 1973 to 1995 over North America except for north-eastern part of Canada. For Eurasia they found increases over China and the Pa-

cific Islands. Over the rest of Eurasia a mixture of positive and negative trends were found, with a tendency for negative trends over eastern Europe and western Russia. Trenberth et al. (2005) found that ocean satellite observations have a positive trend of 0.40 kg/m² in IWV per decade from 1988 to 2003. However, despite a large radiosonde network the temporal resolution is low and differences in calibrations can give systematic errors in humidity. Satellites are able to observe water vapour globally. Some remote sensing methods, observing in the infrared and the optical frequency bands, are limited to clear sky conditions. Other methods, using microwave remote sensing techniques, can be used also during cloudy conditions. On the other hand they only provide high accuracy over oceans. New methods, such as ground-based observations of signals from Global Navigation Satellite Systems (GNSS), can provide IWV observations with high accuracy that complement radiosonde and satellite measurements. As the time series of GNSS data grow longer they can also be used for the detection of trends and other systematic effects. So far, the only GNSS which has provided large amounts of data is the Global Positioning System (GPS).

The advantages of the GNSS measurements are that they are weather independent and have a high temporal resolution. The disadvantage is the limited spatial resolution. The GNSS observations can provide time series of the IWV that can be used to investigate the diurnal and seasonal cycles and to compare with the representation of the water vapour in climate models and help to improve these models. One of the first climate related IWV results inferred from GPS data were made by Gradinarsky et al. (2002) and Elgered et al. (2003) whom showed an increase in the IWV of 7–14% per decade over Scandi-

navia for the time period 1993–2002. More recently Vey et al. (2010) used GPS based IWV data to evaluate the seasonal and inter-annual variations in NCEP model data (NCEP=National Centers for Environmental Prediction of the US Weather Service). They found good agreement except in the tropics and in Antarctica where the NCEP model underestimated IWV by 40 and 25%, respectively.

In this review we focus on the use of ground-based GPS data for a future assessment of the quality of climate models used for simulations of future climate conditions in the region of Fennoscandia. First we summarise the status of climate modelling. Thereafter, we present selected results of IWV time series from Sweden and Finland, e.g., an assessment of the correlation between trends in the IWV with the corresponding trends in the temperature measured close to the ground. We discuss some of the identified systematic errors affecting the long term stability of IWV time series inferred from GPS/GNSS data. The paper is ended by the conclusions.

Status of Climate Models

The climate system involves a large number of processes operating on different temporal and spatial scales. Numerical climate models include descriptions of the most relevant processes and can therefore be used to simulate the climate system including its evolution over time. Simulations for past and present conditions contributes to our understanding of the climate system and causes for climate change. Climate models are also extensively used to simulate the response of the climate system to current and future changes in radiative forcing (e.g. Meehl et al., 2007). Different processes in the climate system can amplify or dampen the climate response to an external perturbation such as the increase in greenhouse gases. The climate sensitivity depend on radiative feed-backs associated with water vapour, lapse rate, clouds, snow, and sea ice, but global estimates of these feed-backs differ among the General Circulation Models (GCMs).

Bony et al. (2006) compared global climate feed-backs for coupled GCMs participating in the IPCC Fourth Assessment Reports (AR4). The water vapour feedback constituted by far the strongest feedback. Their results showed that, the combined water vapour feedback plus the lapse rate feedback amplifies the Earth's global mean temperature response by 40–50%, the surface albedo feedback amplifies it by about 10%, and the cloud feedback amplifies it by 10–50%. Water vapour also takes part in the hydrological cycle by transporting water in the atmosphere and redistributing energy through evaporation and condensation and it affects the precipitation and soil moisture. The vital role of water vapour in the climate system requires that GCMs can represent these atmospheric processes ranging from scales of micrometres up to a few thousands of kilometres. This demands both advanced physical parameterisations of processes on sub-

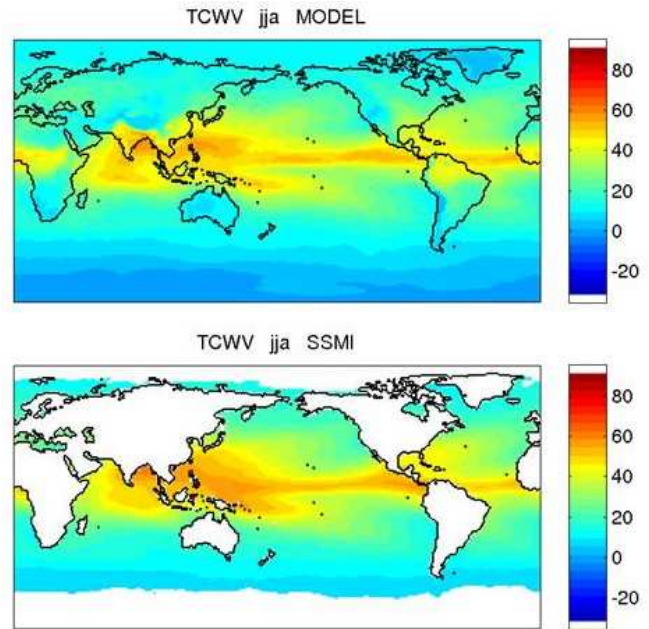


Figure 1: *The vertically integrated water vapour (IWV), for the northern hemisphere summer months of June, July, and August 1990–1992, inferred from (top) the EC-EARTH model, and (bottom) SSM/I observations.*

grid scale as well as high horizontal and vertical resolution to resolve the transport of water in the atmosphere. GCMs typically operate on spatial scales of 100–300 km. The heavy computational demand in long-term climate change simulations implies that they cannot be run at finer resolution, at least not for the large number of simulations required to sample the uncertainties connected to future climate change.

As a means to get to the higher resolution needed for many impact and adaptation studies, regional climate models (RCMs) operating on finer horizontal resolution (typically 10–50 km) are employed (e.g. Rummukainen, 2010). Given appropriate boundary conditions RCMs have been shown to reproduce many important features of the regional/local climate (Christensen et al., 2010).

Many GCMs simulate the evolution of the global mean surface temperature and pressure in the 20th century (Räisänen, 2007). The detailed geographic pattern of change vary between models but the observed changes in temperature, precipitation, and pressure during the last 50 years fall within the range of model results. Other studies (e.g. Johnson & Sharma, 2009) using simulations from several GCMs also find that the best model skill scores are the near-surface variables such as pressure, temperature, and humidity. Confidence in GCM simulated large-scale features of water vapour is relatively high, at least in the boundary layer and in the extra-tropics. Figure 1 depicts an example of the IWV for the climate model EC-Earth (Hazeleger et al., 2010) and from the Special Sensor Microwave/Imager (SSM/I)

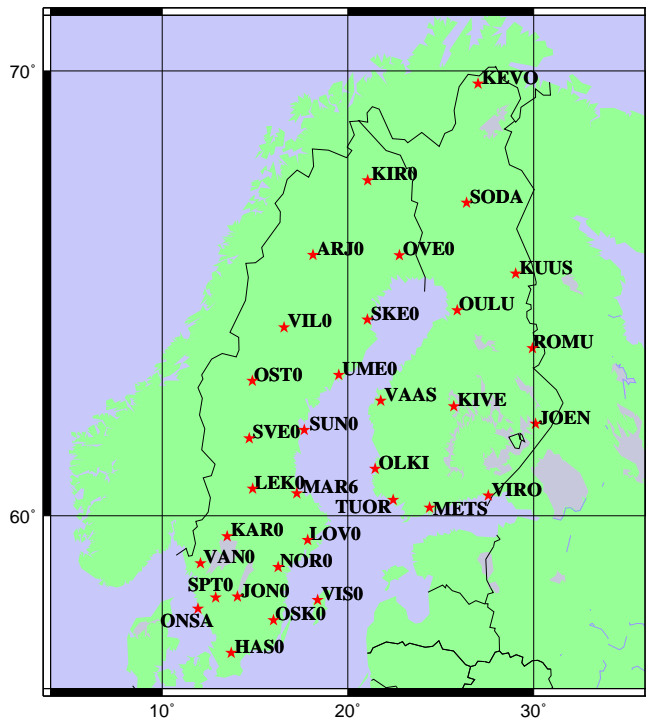


Figure 2: The 33 sites used in the Finnish and Swedish ground-based GNSS networks.

satellite measurements (Wentz & Spencer, 1998).

This also holds true for RCM simulated water vapour, as exemplified for the Arctic by Wyser et al. (1998). In the upper tropical troposphere, on the other hand, confidence in GCM simulated water vapour is lower and this is a region where the water vapour feedback is strong (Randall et al., 2007). Bony et al. (2006) suggest that using new observational data sets, would improve the understanding of the origin of the inter-model differences, and our assessment of the reliability of the climate feedbacks produced by the different GCMs. Apart from serving as input for model evaluation, long-term time series of IWV can be used in order to detect changes in the climate.

Examples of IWV Observations

We use ground-based GPS data acquired at 33 sites: 21 sites in Sweden and 12 sites in Finland during the ten year period from November 17, 1996, to November 16, 2006. Figure 2 depicts the location of the receiver sites and their coordinates are listed in Table 1. The data were processed with the GAMIT/GLOBK version 10.1 software (King, 2002) and provided estimates of the equivalent zenith total delay with a temporal resolution of 2 h (Lidberg et al., 2007). Using model data obtained from the Swedish Meteorological and Hydrological Institute (SMHI), for the ground pressure at these 33 sites, equivalent zenith wet delays were derived and the IWV

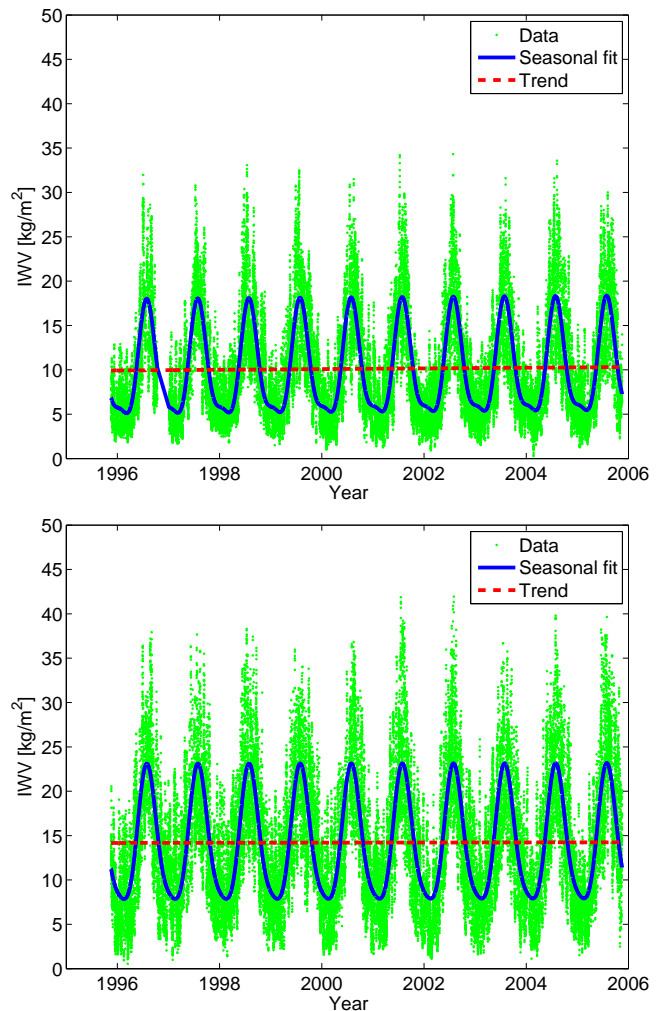


Figure 3: IWV time series from (top) Arjeplog and (bottom) Hässleholm. The original time series of IWV data are denoted by green dots. The periodic function (blue line) is the model in accordance with Equation 1. The dashed red line is the estimated linear trend (from Nilsson & Elgered (2008)).

time series were calculated (Nilsson & Elgered, 2008). Thereafter, linear trends and seasonal components were estimated from the IWV data using the model:

$$V = V_0 + a_1 t + a_2 \sin(2\pi t) + a_3 \cos(2\pi t) + a_4 \sin(4\pi t) + a_5 \cos(4\pi t) \quad (1)$$

where V denotes the IWV; t is the time in years and the model parameters V_0 , a_1 , a_2 , a_3 , a_4 , and a_5 — estimated using the method of least squares — represent a mean value, a linear trend, annual, and semi-annual components. Of specific interest here are the estimated linear trends, a_1 , for the different sites.

Two examples of inferred time series, the Arjeplog site in the north and the Hässleholm site in the south of Sweden, are depicted in Figure 3. We note that due to the

Table 1: *GPS sites and the corresponding observation sites of the ground temperature, sorted by decreasing latitude.*

GPS Site		Longitude [°E]	Latitude [°N]	Height ¹ [m]	Meteorological Site Name	Longitude [°E]	Latitude [°N]	Height ¹ [m]	Distance ² [km]	Height diff. ³ [m]
Acronym	Name									
KEVO	Kevo	27.01	69.76	111	Kevo	27.01	69.76	107	0	4
KIRO	Kiruna	21.06	67.88	469	Kiruna	20.33	67.82	447	31	22
SODA	Sodankylä	26.39	67.42	279	Sodankylä	26.63	67.37	179	11	100
ARJO	Arjeplog	18.13	66.32	459	Arjeplog	17.84	66.05	431	33	28
OVE0	Över Kalix	22.77	66.31	200	Över Kalix	22.85	66.28	61	5	−2
KUUS	Kuusamo	29.03	65.91	361	Kuusamo	29.22	66.00	264	13	97
OULU	Oulu	25.89	65.09	71	Oulunsalo	25.35	64.93	14	31	57
SKE0	Skellefteå	21.05	64.88	59	Luleå	22.13	65.55	17	90	42
VIL0	Vilhelmina	16.56	64.70	420	Gunnarn	17.70	65.00	277	65	143
ROMU	Romuvaara	29.93	64.22	224	Sotkamo	28.34	64.11	161	78	63
UME0	Umeå	19.51	63.58	32	Umeå	20.28	63.80	8	45	24
OST0	Östersund	14.86	63.44	459	Frösön	14.50	63.20	359	32	100
VAAS	Vaasa	21.77	62.96	40	Korsnäs	21.19	62.94	2	29	38
KIVE	Kivetty	25.70	62.82	198	Viitasaari	25.86	63.08	132	30	66
JOEN	Joensuu	30.10	62.39	97	Tohmajärvi	30.35	62.24	90	21	7
SUN0	Sundsvall	17.66	62.23	7	Sundsvall	17.30	62.39	6	26	1
SVE0	Sveg	14.70	62.02	458	Sveg	14.18	62.02	363	27	95
OLKI	Olkiluoto	21.47	61.24	12	Rauma	21.30	61.15	4	14	8
LEK0	Leksand	14.88	60.72	448	Mora	14.51	60.96	196	33	252
MAR6	Mårtsbo	17.26	60.60	51	Gävle	17.16	60.42	16	21	35
VIRO	Virolahti	27.56	60.54	22	Virolahti	27.67	60.53	5	28	17
TUOR	Tuorla	22.44	60.42	41	Kaarina	22.55	60.39	6	7	35
METS	Metsähovi	24.40	60.22	76	Lohja	24.05	60.24	37	19	39
KAR0	Karlstad	13.51	59.44	83	Karlstad	13.33	59.45	100	10	−17
LOV0	Lovö	17.83	59.34	56	Stockholm	18.06	59.34	44	13	12
VAN0	Vänernborg	12.07	58.69	135	Sätenäs	12.72	58.43	54	48	81
NOR0	Norrköping	16.25	58.59	13	Norrköping	16.15	58.58	34	6	−21
JON0	Jönköping	14.06	57.75	227	Jönköping	14.08	57.75	224	1	3
SPT0	Borås	12.89	57.72	185	Borås	12.95	57.76	135	6	50
VIS0	Visby	18.37	57.65	55	Visby	18.35	57.67	47	3	8
ONSA	Onsala	11.93	57.40	9	Nidingen	11.90	57.30	24	11	−15
OSK0	Oskarshamn	16.00	57.06	120	Målilla	15.80	57.38	95	38	25
HAS0	Hässleholm	13.72	56.09	79	Osby	14.00	56.37	82	36	−3

¹The heights are above the mean sea level.

²The distances are calculated assuming the Earth to be a perfect sphere with a radius of 6378.0 km.

³Height differences: (height of GPS site) − (height of meteorological site)

exponential relation between temperature and the saturation pressure of water vapour a simple sine wave is not sufficient to model the seasonal variation. This is more easily seen in the results from the Arjeplog site, where the dry winters are relatively longer. The semi-annual term is therefore larger at this site.

Correlation Between IWV and Temperature

We obtained monthly means of temperatures observed just above the ground at sites nearby to the GPS sites. The sites of the temperature observations are listed in Ta-

ble 1. The temperature data were acquired and archived by the observational networks of the SMHI and the Finnish Meteorological Institute (FMI). We used the same type of six-parameter model as was used in Equation 1 for the IWV. Two examples of the results for the temperature — for the same sites as examined in Figure 3 for the IWV — are depicted in Figure 4. Although we here analyse monthly mean values it is striking how variable the weather conditions (in this case the temperature just above the ground) is from year to year. This implies that it is important to use identical time periods when performing correlation studies between derived parameters, such as between the linear trends for the IWV and for the temperature.

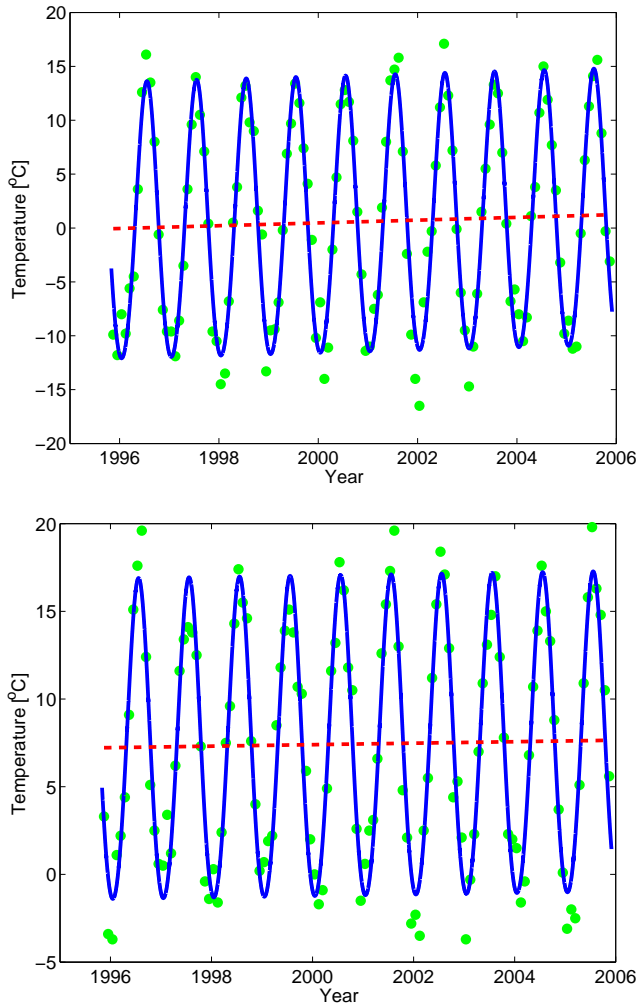


Figure 4: Time series of the monthly means of the temperature at the ground (filled green circles): (top) from Arjeplog and (bottom) from Hässleholm. The periodic function (blue line) is the model in accordance with Equation 1. The dashed red line is the estimated linear trend.

A summary of the comparison between the estimated trends is seen in Figure 5. The IWV trends are presented in the unit percent per decade in order to compare the results to the theoretical expected relation of an increase in the IWV of 6–7% for 1°C increase of the temperature. When examining Figure 5 it is evident that trends are small, both in the temperature and in the IWV in the south-east of Sweden. In Finland sites close to the Baltic Sea have large IWV trends but small temperature trends, while sites to the east have large temperature trends but small IWV trends. This means that there is a negative correlation between temperature and IWV trends in the south and middle of Finland. On the other hand, the two most northern sites in Finland show trend results that are more consistent with the positive correlation seen for most of the sites in Sweden.

In order to further study these results, a correlation plot between the estimated linear trends is shown in Fig-

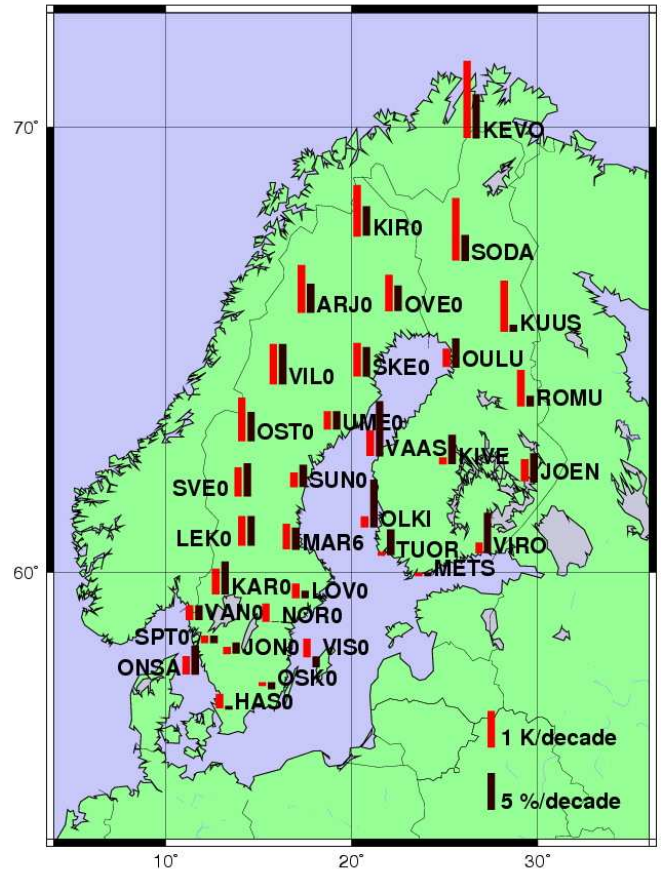


Figure 5: Estimated linear trends in the IWV and in the temperature close to the ground for the Swedish and the Finnish sites. The scales of the bars are defined in the lower right corner.

ure 6. As seen from the figure the linear slopes of the best fitted linear relations are significantly different for the Swedish and the Finnish sites. For the Swedish sites we obtain a slope of 3.9 %/K whereas the slope is 0.0 %/K for the Finnish sites. Using all sites the slope obtained is 2.1%/K. All these values are far from the expected global mean of 6–7%/K. This shall not necessarily cause too much concern given that the studied region is very small in a global perspective and in terms of estimating average trends the time series are acquired over a very short time period. Furthermore, the experimental evidence presented in support for a slope of 6–7%/K are mainly from the equatorial region (Trenberth et al., 2003).

For the time being we cannot conclude if the differences seen are due to different weather conditions in Sweden and Finland for this time period, or if there are systematic differences in the acquired GPS data. After all, the number of sites studied are small and in a statistical sense many more stations would be extremely useful for further assessment of these results.

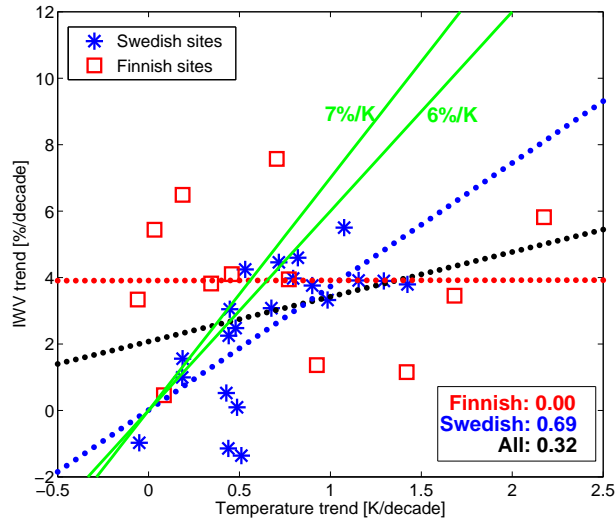


Figure 6: Correlation between trends in ground temperature and IWV for the 33 sites. The correlation obtained for the Swedish sites (blue stars) is significant, whereas the correlation for the Finnish sites (red squares) is actually zero. Also included in the graph are the theoretical relations of 6 and 7% increase in the IWV for each degree increase in temperature (green solid lines).

Assessment of Systematic Errors

Several sources of systematic errors of the GNSS technique that have an impact on estimates of the IWV are identified. For example, the different models of geophysical phenomena such as Earth tides and loading effects on the crust of the Earth have their own inherent accuracies. Systematic effects are also introduced by the so called mapping functions, which model the elevation dependence of the different propagation delays caused by the atmosphere and are used in the data processing when estimating the equivalent zenith total delays. Here, however, we present a couple of results related to systematic effects caused by the antennas and the electromagnetic environment around them.

In order to optimally determine the IWV, a correct model of the received signal phase is essential. Most unmodelled signal phase phenomena that are elevation dependent have a large influence on both the vertical coordinate of the position estimate and the estimate of the signal delay due to the atmosphere, which in turn maps to the IWV values. Jarlemark et al. (2010) investigated how satellite antenna phase centre variations, local electromagnetic properties of the antennas, influence IWV estimates.

Figure 7 shows antenna phase centre variations for the three GPS satellite types presently in use, i.e., II/IIA, IIR-A, and IIR-B/M. These phase variations at the satellite antenna are observed as elevation dependent addi-

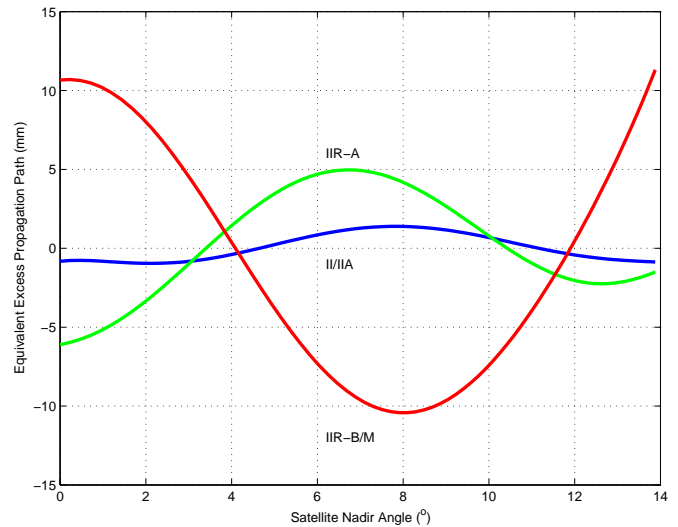


Figure 7: Antenna phase center variations vs. the nadir angle from the GPS satellite to the ground receiver for the three satellite types II/IIA (blue), IIR-A (green), and IIRB/M (red) (from Jarlemark et al. (2010)).

tional phase delays at the receiving antenna.

The amplitude of the variations is larger for the satellites of type IIR-B/M. The number of satellites of this type has steadily increased during the period from 2003 to 2008, from 0 to 10 satellites. We find that ignoring the phase variations of the satellite antenna in the processing of the GPS data for this time period can lead to an additional IWV trend of about $0.15 \text{ kg/m}^2/\text{year}$. This value roughly corresponds to $10\%/decade$, which is larger than any of the estimated trends. We note, however, that this is an upper limit obtained when selecting a relatively short time period (six years) with the largest sensitivity to this systematic effect.

Another systematic effect is the electromagnetic environment of the receiving antenna. Systematic studies have been carried out at the Onsala site using an experimental GPS receiver site, located just 12 m from the IGS site ONSA which is used as a reference. The different geometries are shown in Figure 8. The impact of using microwave absorbing material, ECCOSORB, below the antenna was found to have the largest and a significant impact (Ning et al., 2011). It affected the offset in the IWV, which decreased from 1.6 to 0.3 kg/m^2 when compared to results from the IGS site ONSA. This decrease was expected since the IGS site has a similar arrangement using ECCOSORB below the antenna.

The use of a hemispherical radome, compared to having no radome at all, implied no significant impact in the estimated amount of the IWV ($< 0.4 \text{ kg/m}^2$). Additional measurement campaigns are needed in order to reduce the uncertainties further. Due to the relative large variations in the weather it is difficult to compare the quality of atmospheric estimates that are obtained dur-



Figure 8: *Experimental setups for assessment of the impact of adding microwave absorbing material (ECCOSORB) and/or using a hemispheric radome (from Ning et al. (2011)). Sessions A, B, and C use a radome. Sessions C and D use ECCOSORB below and around the antenna. Sessions E and F use ECCOSORB below the antenna only.*

ing different time periods. Ideally several close antenna monuments shall be used where radomes are installed and removed, or interchanged, in a random fashion over a long time period — at least many months. Using such an arrangement the comparisons are performed with identical weather conditions.

Conclusions

GNSS are capable of monitoring the Integrated atmospheric Water Vapour (IWV) with high accuracy over long time scales, but systematic errors cannot be ignored. This is especially true when we, as in this case, are studying small trends in the IWV, and are trying to draw conclusions concerning the relation between these trends and other climate parameters. Because of the variability of the weather over time scales of several years, studies using time series from different periods result in values of trends, as well as correlations, which are not stable. Nevertheless, the results are consistent in many aspects. Nearby sites show similar characteristics and IWV trends are reasonable. As the time series of ground-based GNSS data become longer, it will be possible to assess systematic errors as well as true atmospheric signals (e.g. trends) in more detail. These future studies of course include a continued assessment of the contradicting results obtained concerning the correlation between the estimated trends in temperature and IWV for the different studied regions.

Acknowledgements

We are grateful to the support from the operators of the ground-based GNSS networks: Lantmäteriet in Sweden and the Finnish Geodetic Institute in Finland. The monthly means of temperature for the Finnish sites were kindly provided by Reima Eresmaa at the Finnish Meteorological Institute. This research is supported by VINNOVA, the Swedish Governmental Agency for Innovation Systems, through the project P29459-1 “Long Term Water Vapour Measurements Using GPS for Improvement of Climate Modelling”.

References

- Bengtsson, L. (2010): The global atmospheric water cycle. *Environ. Res. Lett.*, **109**, doi: 10.1088/1748-9326/5/025002.
- Bony, S., Colman, R., Kattsov, V. M., Allan, R. P., & et al. (2006): How well do we understand and evaluate climate change feedback processes? *J. Clim.*, **19**(15), 3445–3482.
- Christensen, J., Kjellström, E., Giorgi, F., Lenderink, G., & Rummukainen, M. (2010): Weight assignment in regional climate models. *Climate Res.*, **44**(2–3), 179–194.
- Elgered, G., Stoew, B., Gradinarsky, L., & Bouma, H. (2003): Analysis of atmospheric parameters derived

- from ground-based GPS observations. In *Proceedings of the International Workshop on GPS Meteorology, Tsukuba, Japan*, edited by R. A. E. A. Anthes, pp. 3–11, Japan Int. Sci. and Technol. Exchange Cent.
- Gradinarsky, L. P., Johansson, J., Bouma, H. R., Scherneck, H.-G., & Elgered, G. (2002): Climate monitoring using GPS. *Phys. Chem. Earth*, **27**, 335–340.
- Hazeleger, Severijns, W. J. C., Semmler, T., Stefanescu, S., Yang, S., Wang, X., Wyser, K., Baldasano, J. M., R. Bintanja, P. B., Caballero, R., Dutra, E., Ekman, A. M. L., Christensen, J. H., van den Hurk, B., Jimenez, P., Jones, C., Källberg, P., Koenigk, T., McGrath, R., Miranda, P., van Noije, T., Parodi, J. A., Schmith, T., Selten, F., Storelmo, T., Sterl, A., Tapamo, H., Vancoppenolle, M., Viterbo, P., & Willén, U. (2010): EC-Earth: a seamless earth system prediction approach in action. *Bull. Am. Meteorol. Soc.*, **91**, 1357–1363.
- Jarlemark, P. O. J., Emardson, R., Johansson, J. M., & Elgered, G. (2010): Ground-based GPS for validation of climate models: the impact of satellite antenna phase center variations. *IEEE Trans. Geosci. Rem. Sens.*, **GE-43**, 1028–1035, doi: 10.1029/2001GL014568.
- Johnson, F. & Sharma, A. (2009): Measurement of GCM skill in predicting variables relevant for hydroclimatological assessments. *J. Climate*, **22**, 4373–4382.
- King, R. (2002): Documentation for the GAMIT GPS analysis software. Internal report, MIT, <http://www.gpsg.mit.edu/simon/gtgk/GAMIT.pdf>.
- Lidberg, M., Johansson, J. M., Scherneck, H.-G., & Davis, J. L. (2007): GPS-derived 3D velocity field of the glacial isostatic adjustment (GIA) in Fennoscandia. *J. Geod.*, **81**, 213–230, doi:10.1007/s00190-006-0102-4.
- Meehl, G., Stocker, T., Collins, W., Friedlingstein, P., Gaye, A., Gregory, J., Kitoh, A., Knutti, R., Murphy, J., Noda, A., Raper, S., Watterson, I., Weaver, A., & Zhao, Z.-C. (2007): Global climate projections. In *Climate Change 2007: The Physical Science Basis. Contribution of Working Group I to the Fourth Assessment Report of the Intergovernmental Panel on Climate Change*, edited by S. Solomon, D. Qin, M. Manning, Z. Chen, M. Marquis, K. Averyt, M. Tignor, & H. Miller, Cambridge University Press, Cambridge, United Kingdom and New York, NY, USA.
- Nilsson, T. & Elgered, G. (2008): Long-term trends in the atmospheric water vapor content estimated from ground-based GPS data. *J. Geophys. Res.*, **113**, doi: 10.1029/2008JD010110.
- Ning, T., Elgered, G., & Johansson, J. (2011): The impact of microwave absorber and radome geometries on GNSS measurements of station coordinates and atmospheric water vapour. *J. Adv. Space Res.*, **47**, 186–196, doi:10.1016/j.asr.2010.06.023.
- Räisänen, J. (2007): How reliable are climate models? *Tellus*, **59A**, 2–29.
- Randall, D., Wood, R., Bony, S., Colman, R., Fife, T., Fyfe, J., Kattsov, V., Pitman, A., Shukla, J., Srinivasan, J., Stouffer, R., Sumi, A., & Taylor, K. (2007): Climate models and their evaluation. In *Climate Change 2007: The Physical Science Basis. Contribution of Working Group I to the Fourth Assessment Report of the Intergovernmental Panel on Climate Change*, edited by S. Solomon, D. Qin, M. Manning, Z. Chen, M. Marquis, K. Averyt, M. Tignor, & H. Miller, Cambridge University Press, Cambridge, United Kingdom and New York, NY, USA.
- Ross, R. J. & Elliott, W. P. (1996): Tropospheric water vapor climatology and trends over north america: 1973–93. *J. Climate*, **9**, 3561–3574.
- Ross, R. J. & Elliott, W. P. (2001): Radiosonde based northern hemisphere tropospheric water vapor trends. *J. Climate*, **14**, 1602–1612.
- Rummukainen, M. (2010): State-of-the-art with regional climate models. *Wiley Interdisciplinary 2 Reviews: Climate change*, **1**(1), 82–96.
- Trenberth, K. E., Dai, A., Rasmussen, R. M., & Parsons, D. B. (2003): The changing character of precipitation. *Bull. Amer. Meteor. Soc.*, **84**(9), 1205–1217, doi: 10.1175/BAMS-84-9-1205.
- Trenberth, K. E., Fasullo, J., & Smith, L. (2005): Trends and variability in column-integrated atmospheric water vapor. *Climate Dyn.*, **24**, 741758.
- Vey, S., Dietrich, R., Rlke, A., Fritsche, M., Steigenberger, P., & Rothacher, M. (2010): Validation of precipitable water vapor within the NCEP/DOE reanalysis using global GPS observations from one decade. *J. Climate*, **23**, 1675–1695, doi: 10.1175/2009JCLI2787.1.
- Wentz, F. J. & Spencer, R. W. (1998): SSM/I rain retrievals within a unified all-weather ocean algorithm. *J. Atmos. Sci.*, **55**, 1613–1627.
- Wyser, K., Jones, C. G., Du, P., Girard, E., U., W., Casano, J., Christensen, J. H., Curry, J. A., Dethloff, K., Haugen, J.-E., Jacob, D., Költzow, M., Laprise, R., Lynch, A., Pfeifer, S., Rinke, A., Serreze, M., Shaw, M. J., Tjernström, M., & Zagar, M. (1998): An evaluation of arctic cloud and radiation processes during the sheba year: Simulation results from 8 arctic regional climate models. *Climate Dynamics*, **30**, 203223, D09207, doi: 10.1029/2004JD004751.